Tiling and somatotopic alignment of mammalian low-threshold mechanoreceptors

Emily D. Kuehn[a,b,c,d,1,2], Shan Meltzer[a,b,1], Victoria E. Abraira[a,b,3], Cheng-Ying Ho[c,d,4], and David D. Ginty[a,b,5]

[a]Department of Neurobiology, Harvard Medical School, Boston, MA 02115; [b]Howard Hughes Medical Institute, Harvard Medical School, Boston, MA 02115; [c]Solomon H. Snyder Department of Neuroscience, The Johns Hopkins University School of Medicine, Baltimore, MD 21205; and [d]Howard Hughes Medical Institute, The Johns Hopkins University School of Medicine, Baltimore, MD 21205

This contribution is part of the special series of Inaugural Articles by members of the National Academy of Sciences elected in 2017.

Contributed by David D. Ginty, March 15, 2019 (sent for review January 24, 2019; reviewed by Wesley Grueber and Baldomero M. Olivera)

Innocuous mechanical stimuli acting on the skin are detected by sensory neurons, known as low-threshold mechanoreceptors (LTMRs). LTMRs are classified based on their response properties, action potential conduction velocity, rate of adaptation to static indentation of the skin, and terminal anatomy. Here, we report organizational properties of the cutaneous and central axonal projections of the five principal hairy skin LTMR subtypes. We find that axons of neurons within a particular LTMR class are largely nonoverlapping with respect to their cutaneous end organs (e.g., hair follicles), with Aβ rapidly adapting-LTMRs being the sole exception. Individual neurons of each LTMR class are mostly nonoverlapping with respect to their associated hair follicles, with the notable exception of C-LTMRs, which exhibit multiple branches that redundantly innervate individual hair follicles. In the spinal cord, LTMR central projections exhibit rostrocaudal elongation and mediolateral compression, compared with their cutaneous innervation patterns, and these central projections also exhibit a fine degree of homotypic topographic adjacency. These findings thus reveal homotypic tiling of LTMR subtype axonal projections in hairy skin and a remarkable degree of spatial precision of spinal cord axonal termination patterns, suggesting a somatotopically precise tactile encoding capability of the mechanosensory dorsal horn.

somatosensation | mechanosensory | tiling | somatotopy

Sensory systems encode salient features of the external world, enabling animals to thrive within their environmental niches. For the somatosensory system, the principal conduit to the external world is through the skin. Understanding of the organization of low-threshold mechanoreceptors (LTMR) cutaneous receptive fields with respect to their projective fields in the spinal cord is fundamental to any model of early somatosensory processing.

The somatosensory system allows animals to perceive and react to a range of stimuli impinging on the skin, including indentation and stretch of the skin, skin vibration, and contact with body hairs and other skin appendages, such as whiskers, feathers, spines, and fingernails. Innocuous mechanical stimuli are detected by LTMRs, which are a diverse group of sensory neurons endowed with distinct peripheral and central morphologies, sensitivities, and physiological properties (1, 2). The cell bodies of mammalian LTMRs reside within dorsal root ganglia (DRG) and trigeminal ganglia; these neurons extend one axonal branch to the skin (2, 3) and another to the spinal cord dorsal horn and, in some cases, the brainstem (1).

Mammalian cutaneous LTMRs are classified as either Aβ, Aδ, or C based on their action potential-conduction velocities (4). They are further distinguished by their rates of adaptation to sustained indentation of the skin (5) and their sensitivity to various mechanical stimuli. The latter is determined, at least in part, by the cutaneous end organs with which LTMR subtypes associate (2), as well as distinguishing intrinsic molecular and physiological properties. At least five physiologically distinct LTMR subtypes innervate mammalian hairy skin (Fig. 1). These are: Aβ slowly adapting (SA)-LTMRs, which associate with clusters of Merkel cells, or touch domes, in the basal epidermis; Aβ rapidly adapting (RA)-LTMRs, Aδ-LTMRs, and C-LTMRs, each of which form longitudinal lanceolate endings associated with hair follicles; and Aβ Field-LTMRs, which form circumferential endings that wrap around hair follicles, surrounding the lanceolate ending complexes (2, 6). While Aβ RA-LTMRs, Aδ-LTMRs, and C-LTMRs are sensitive to both gentle skin indentation and deflection of hairs, Aβ SA-LTMRs respond to skin indentation but not hair deflection (2). Aβ Field-LTMRs are sensitive to stroking across the skin, but not to hair deflection and typically to indentation only in the high-threshold range (6). These five hairy skin LTMR subtypes are observed in all mammals examined, ranging from mice to cats to humans.

The mouse (*Mus musculus*) has proven to be a valuable model organism for understanding the neurophysiological and morphological properties of the five hairy skin LTMR subtypes and their functions in somatosensation, at least in part because of the availability of genetic tools to label and visualize these neurons. In mouse hairy skin, each LTMR subtype exhibits an intimate relationship with one or more of the three principal hair follicle types found in mice trunk hairy skin: guard, awl/auchene, and

Significance

The sense of touch is essential for perceiving the physical world, sensory-motor control, and social exchange. The first step of touch perception is activation of low-threshold mechanoreceptor (LTMR) neurons that innervate the skin. LTMRs extend one axonal branch to the skin and another to the spinal cord dorsal horn. There exist at least five LTMR subtypes that innervate mouse hairy skin, each with distinct morphologies, response properties, and presumably functions. We used genetic labeling and whole-mount visualization strategies to reveal spatial relationships between axons of individual LTMRs across 2D areas of skin and the extent to which these relationships are topographically arranged within the 3D space of the spinal cord, uncovering organizational principles of the mammalian tactile sensory system.

Author contributions: E.D.K., S.M., V.E.A., C.-Y.H., and D.D.G. designed research; E.D.K., S.M., V.E.A., C.-Y.H., and D.D.G. performed research; E.D.K., V.E.A., C.-Y.H., and D.D.G. contributed new reagents/analytic tools; E.D.K., S.M., V.E.A., C.-Y.H., and D.D.G. analyzed data; and E.D.K., S.M., and D.D.G. wrote the paper.

Reviewers: W.G., Columbia University; and B.M.O., University of Utah.

The authors declare no conflict of interest.

[1]E.D.K. and S.M. contributed equally to this work.

[2]Present address: Department of Science Education and Strategic Communications, Walter Reed Army Institute of Research, Silver Spring, MD 20910.

[3]Present address: Department of Cell Biology and Neuroscience, Rutgers University, New Brunswick, NJ 08854-8000.

[4]Present address: Department of Pathology, University of Maryland School of Medicine, Baltimore, MD 21201.

[5]To whom correspondence should be addressed. Email: david_ginty@hms.harvard.edu.

This article contains supporting information online at www.pnas.org/lookup/suppl/doi:10.1073/pnas.1901378116/-/DCSupplemental.

Published online April 17, 2019.

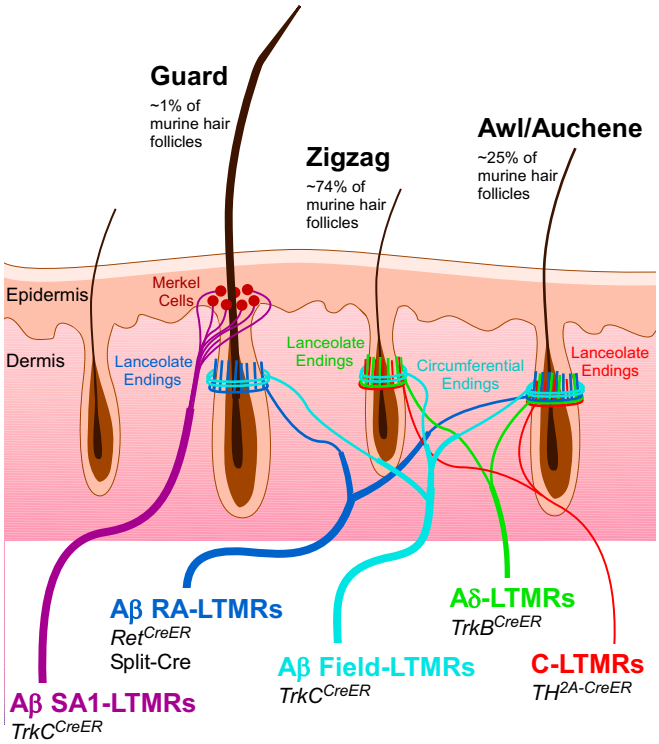

Fig. 1. Summary schematic of known murine LTMR types and their respective innervation patterns in hairy skin. Aβ SA1-LTMRs (purple) associate with clusters of Merkel cells at the base of guard hairs; Aβ RA-LTMRs (dark blue) form longitudinal lanceolate endings associated with guard and awl/auchene hairs; Aδ-LTMRs (green) and C-LTMRs (red) form longitudinal lanceolate endings associated with zigzag and awl/auchene hairs; Aβ Field-LTMRs form circumferential endings that wrap around hair follicles, surrounding the lanceolate ending complexes, on all hair types. Murine genetic tools used in this study to target each specific LTMR subtype are noted, and are further detailed in *SI Appendix*, Table S1.

zigzag hair follicles (Fig. 1). Guard hairs, which account for ∼1% of trunk skin hairs and are the longest, are innervated by Aβ RA-LTMRs lanceolate endings and surrounding Aβ Field-LTMRs circumferential endings and are also associated with Aβ SA type I (SAI)-LTMRs/Merkel cell complexes (1, 5, 7, 8). Awl/auchene hair follicles, which account for ∼25% of hairs, are triply innervated by Aβ RA-LTMRs, Aδ-LTMRs, and C-LTMR lanceolate endings that terminate in a striking, interdigitated manner (9), and are surrounded by Aβ Field-LTMR circumferential endings (6). Zigzag hair follicles, the most abundant hair follicle type, are innervated by interdigitated lanceolate endings of Aδ-LTMRs and C-LTMRs and the surrounding circumferential endings of Aβ Field-LTMRs (1, 5, 7, 8). The majority of hair follicles are also innervated by lightly myelinated high-threshold mechanosensory neurons that express the peptide CGRP which, like Aβ Field-LTMRs, form circumferential endings surrounding the lanceolate complexes and respond to hair pull (6, 10). Each of the three principal hair follicle types of mouse hairy skin is thus neurophysiologically distinct.

The identification of five LTMR subtypes that form unique terminal morphologies and spatial patterns of innervation of mouse hairy skin raises questions about how their cutaneous endings are organized relative to one another. In the fly, *Drosophila melanogaster*, the peripheral endings of mechanosensory neurons of the same class exhibit minimal overlap in the body wall, a phenomenon known as "tiling" (11). Moreover, individual branches of each *Drosophila* mechanosensory neuron displays minimal overlap; developing isoneuronal branches repel each other to establish this spatial arrangement. This phenomenon is termed "self-avoidance" (12). Both tiling and self-avoidance are observed in many systems and neuronal types across species, including sensory neurons in *Caenorhabditis elegans*, *Drosophila*, and zebrafish, as well as mammalian cerebellar Purkinje cells and retinal neuron types (12–19). It is believed that tiling and self-avoidance exist in sensory systems to ensure complete and nonredundant coverage of sensory space. Whether the five mammalian LTMRs that innervate hairy skin exhibit tiling and features of self-avoidance is currently unknown.

Deciphering how and where the periphery is represented in the CNS is crucial for understanding the organizational logic of sensory systems. As with the mammalian auditory and visual systems, the somatosensory system is topographically organized, with internal representations of the body surface in the spinal cord, brainstem, tectum, thalamus, and somatosensory cortex (20–26). In these CNS areas, somatotopic maps, while disproportionate, are arranged such that neighbor relationships in the periphery are generally maintained, although central representation areas are often discontinuous. Consistent with this, the central axonal projections of hairy skin LTMR subtypes overlap in the deep dorsal horn while remaining topographically organized (7, 27). However, the precise positioning of spinal cord terminations of individual LTMRs of any of the five hairy skin LTMR classes whose receptive fields are immediately adjacent or overlapping in the periphery is not known. Thus, determining the extent of tiling and self-avoidance of LTMR peripheral projections within the 2D area of the skin and how the central terminals of individual LTMRs of a given class are arranged within the 3D space of the spinal cord will inform models of touch representation and processing within the CNS.

Here, we sought to determine the degree of tiling and isoneuronal overlap of axonal endings in the skin, as well as organizational properties of the central projections of the five principal hairy skin LTMR subtypes of the mouse. Using LTMR genetic labeling strategies that we have amassed over the last decade (6–8, 27–29) and whole-mount staining of the skin, we achieved multicolor labeling of peripheral sensory neurons, and found that peripheral receptive fields of the majority of LTMR subtypes are predominantly tiled (nonoverlapping) with respect to the hair follicles they innervate, with Aβ RA-LTMRs being the sole exception. Furthermore, cutaneous axonal branches that arise from individual LTMRs show variable degrees of isoneuronal overlap: among four hair follicle-innervating LTMR subtypes, individual Aβ Field-LTMRs and Aβ RA-LTMRs exhibit the lowest degree of isoneuronal axonal overlap or contact, a feature of self-avoidance. Centrally, the projections of each LTMR subtype exhibit expansion along the rostrocaudal axis and compression within the mediolateral axis, relative to the skin regions covered by their respective peripheral projections. Moreover, sparse multicolor labeling strategies revealed that LTMRs display central terminations within the dorsal horn LTMR-recipient zone (RZ) that exhibit remarkably precise overlap or adjacency. Some body region-specific differences in LTMR peripheral and central projection patterns are noted. Thus, the majority of mammalian LTMRs exhibit uniform, tiled patterns of hairy skin innervation, and a striking, previously unappreciated high degree of somatotopic precision within the initial tactile information processing region of the CNS, the mechanosensory dorsal horn.

Results

Most Hairy Skin LTMR Subtypes Tile the Skin. LTMRs innervate mammalian hairy skin in highly stereotyped patterns (7); however, little is known about the relationships between the peripheral endings of individual, neighboring neurons within an LTMR class. To visualize the relationships between individual neurons within an LTMR class, at a population level, we used a combination of LTMR-CreER mouse genetic tools (Fig. 1 and *SI Appendix*, Table S1) and two orthogonal Cre-recombinase–dependent fluorescent reporters, Ai3 and Ai9 (30). Using two

reporters in the same mouse in combination with LTMR-CreER lines permits multicolor labeling of one particular LTMR population in a stochastic fashion: some neurons within the same class are labeled with tdTomato (Ai9), some with YFP (Ai3), and some with both tdTomato and YFP. Thus, treatment with an optimal tamoxifen dosage achieves labeling of the majority of neurons of a particular LTMR subtype in one of three colors at comparable ratios (~one-third red, ~one-third green, ~one-third yellow) (*SI Appendix*, Fig. S1 and Fig. 2*A*). Combining this labeling strategy with a whole-mount fluorescent staining preparation of the skin allowed us to visualize and quantify the number of neurons innervating individual hair follicles and to assess the extent of overlap of the cutaneous projections of individual LTMRs of a given class (Fig. 2 *B*–*F*). We observed that the majority of LTMR classes exhibit largely nonoverlapping association with their respective peripheral-end organs; C-LTMRs, Aδ-LTMRs, Aβ SAI-LTMRs, and Aβ Field-LTMRs displayed single-neuron innervation of >70% of the hair follicles with which they associate (Fig. 2*G*). Aβ RA-LTMRs are the only subtype for which two or more individual neurons often innervate the same hair follicle. In fact, many Aβ RA-LTMRs displayed triple hair follicle innervation, and fewer than half of the follicles innervated showed a single-neuron innervation pattern (Fig. 2*G*). It is noteworthy that while Aβ Field-LTMRs display single-neuron innervation of >90% of the hair follicles, the receptive fields of individual Aβ Field-LTMRs overlap extensively to innervate distinct groups of hair follicles within overlapping skin areas (Fig. 2*D*, *Insets*). This reveals an interesting and distinguishing feature of Aβ Field-LTMRs. While C-LTMRs, Aδ-LTMRs, Aβ SAI-LTMRs, and to a lesser extent Aβ RA-LTMRs, are tiled with respect to both the hair follicles with which they associate and skin regions, Aβ Field-LTMRs are tiled with respect to hair follicles, but are overlapping with respect to the hairy skin regions they innervate.

Across the body, skin regions exhibit differences in elasticity, barrier properties, and expression of proteins, such as androgen receptors (31–33). Furthermore, the three main hair follicle types are present in different mouse hairy skin regions at varying ratios and these hairs receive unique patterns of LTMR subtype-specific innervation. As such, different skin regions may be tasked with unique sensory functions and may have different patterns of LTMR innervation. Therefore, we speculated that different patterns of peripheral innervation by LTMR subtypes according to body location or hair follicle type might exist. We assessed the extent of overlap of LTMR subtype peripheral receptive fields according to body region and the hair follicle types being innervated. This latter analysis utilized the presence of Troma1$^+$ Merkel cell clusters, which form exclusively around the necks of guard hairs (7) to distinguish guard hairs from zigzag and awl/auchene hairs. Of the five LTMR subtypes, only Aβ SAI-LTMRs exhibited a difference in their extent of overlap according to body region, with a higher incidence of dual innervation of Merkel cell complexes associated with guard hairs of abdominal hairy skin (Fig. 3*A*). Aβ RA-LTMRs and Aβ Field-LTMRs are the only two LTMR populations that innervate both guard hairs and awl/auchene or zigzag hairs, and for both of these LTMR populations, guard hairs were observed to receive a higher incidence of dual (or triple, in the case of Aβ RA-LTMRs) innervation than other hair follicle types (Fig. 3*B*). In fact, all guard hairs were innervated by either two or three Aβ RA-LTMRs whose lanceolate endings around follicles were often partitioned but sometimes interdigitated (Fig. 2*F*, *Lower Inset*). Thus, while most LTMR peripheral projections are tiled with respect to hair follicles across hairy skin, some body regions and hair follicle types exhibit double or even triple innervation from select LTMR subtypes.

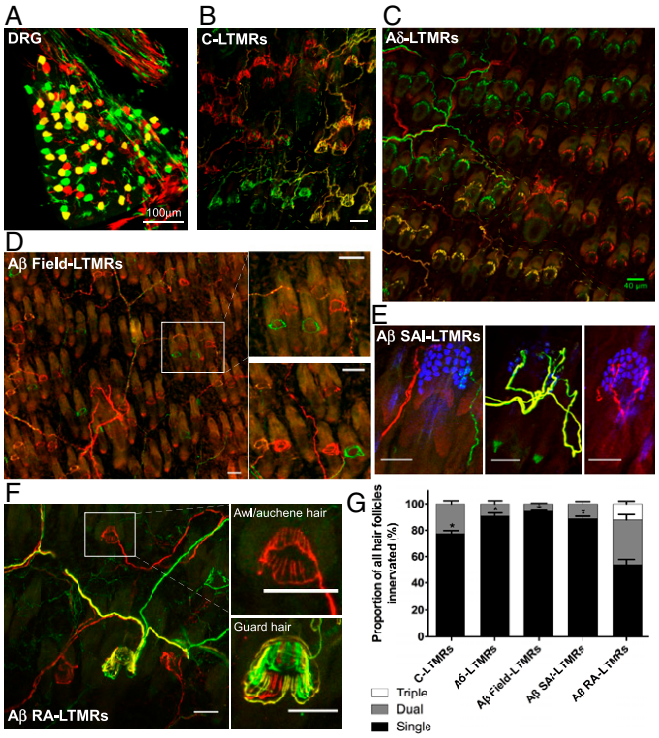

Fig. 2. LTMR peripheral receptive fields are largely nonoverlapping. (*A*) Representative image of whole-mount DRG (*TrkB*^{CreER};Ai3/Ai9), showing ~33% green, ~33% red, and ~33% yellow stochiometric labeling of LTMR neurons (in this case, Aδ-LTMRs). Similar images for all LTMR subtypes and labeling efficiency quantifications may be found in *SI Appendix*, Fig. S1. *B*–*F* are representative images from hairy skin whole-mount immunostaining (Ai3, green; Ai9, red; Troma1$^+$ Merkel cells, blue) of (*B*) C-LTMRs, (*C*) Aδ-LTMRs, (*D*) Aβ Field-LTMRs, (*E*) Aβ SAI-LTMRs, and (*F*) Aβ RA-LTMRs. (Scale bars, 50 μm unless otherwise noted.) Tracings in *B* and *C* (C-LTMRs and Aδ-LTMRs, respectively) highlight the boundaries of individual neurons, showcasing the tiled organization of these LTMR subtypes with respect to both skin region and individual hair follicles. Aβ Field-LTMRs (*D*) lack this tiled organization with respect to skin region, showing single neuron innervation of individual hair follicles, but in an interspersed innervation pattern, as highlighted in the *Insets*. The three examples of Aβ SAI-LTMRs in *E* showcase a rare example of dual innervation and two examples of single-neuron innervation of Troma1$^+$ Merkel cell complexes. The *Insets* of *F* showcase the diversity of Aβ RA-LTMR innervation patterns, with single innervation common for awl/auchene hairs (*Upper*), and triple innervation frequently observed in guard hairs (*Lower*). (*G*) Quantifications of relative peripheral overlap of individual neurons for each LTMR subtype. Of the total hair follicles innervated by each LTMR subtype, bars indicate the relative fraction that receive single (black), dual (dark gray), or triple (white) innervation by that subtype. Genotypes, tamoxifen treatments, and number of animals used: C-LTMRs [0.07 mg tamoxifen at postnatal day (P)16 to *TH*$^{2A\text{-}CreER}$;Ai3/Ai9, $n = 5$ animals]; Aδ-LTMRs [3 mg at embryonic day (E)12.5 to *TrkB*^{CreER};Ai3/Ai9, $n = 4$ animals]; Aβ Field-LTMRs (2 mg at E16.5 to *TrkC*^{CreER};Ai3/Ai9, $n = 4$ animals); Aβ SAI-LTMRs (2 mg at E12.5 to *TrkC*^{CreER};Ai3/Ai9, $n = 5$ animals); and Aβ RA-LTMRs (2 mg at E11.5 to E12.5 to *Ret*^{CreER}Ai3/Ai9, $n = 3$ animals). A one-sample *t* test was used to determine if proportion of single innervation was greater than 70%; significance is indicated above the respective bar graph (*$P < 0.05$).

Peripheral Axons of Individual LTMRs Are Largely Nonoverlapping. We next focused on the cutaneous morphological properties of individual neurons within each LTMR class to assess the extent to which axons of individual neurons overlap with respect to the hair follicles they innervate. For this "isoneuronal" analysis, we used a sparse genetic labeling strategy, combining LTMR-CreER mouse genetic tools (Fig. 1 and *SI Appendix*, Table S1) with a Cre-dependent alkaline phosphatase (AP) reporter (34) to visualize the axons of individual neurons. Treatment with a low

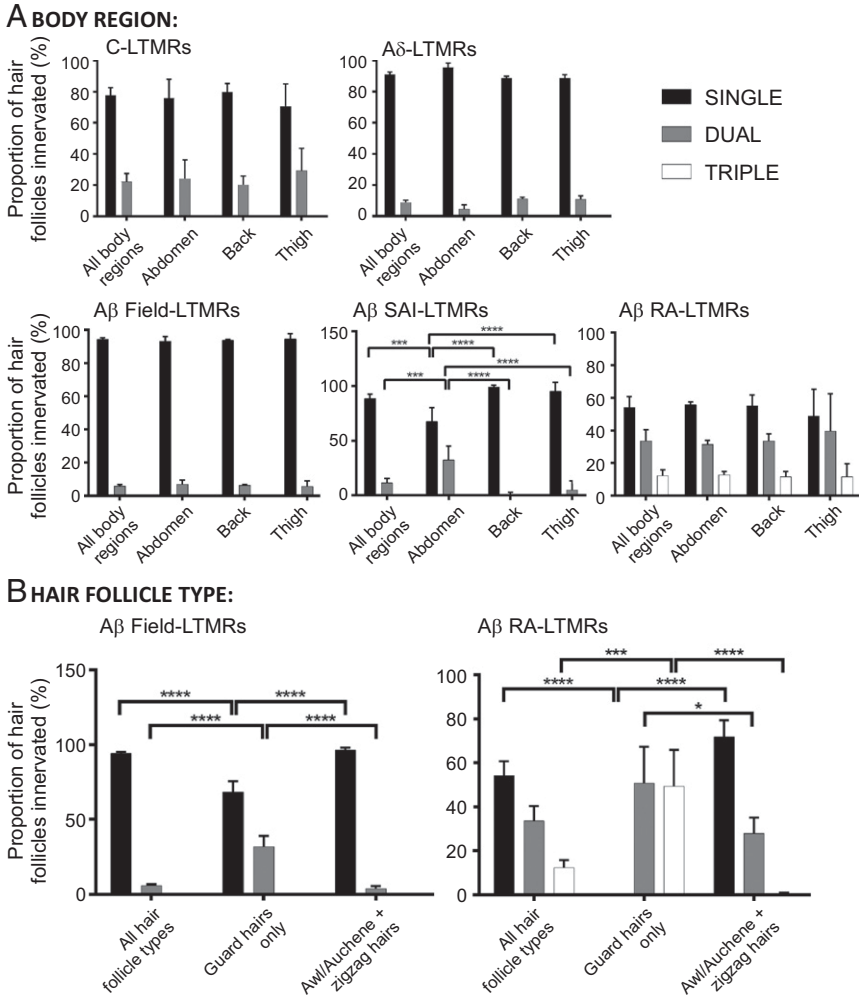

Fig. 3. LTMR peripheral receptive field overlap patterns differ according to body region or hair follicle type. Quantifications of relative peripheral overlap within specific LTMR subpopulations according to (*A*) body region or (*B*) hair follicle type. Of the total hair follicles innervated by each LTMR subtype, bars indicate the relative fraction that receive single (black), dual (gray), or triple (white) innervation from that subtype. C-LTMRs (0.07 mg tamoxifen at P16 to $TH^{2A\text{-}CreER}$;Ai3/Ai9, $n = 3$ animals), Aδ-LTMRs (3 mg at E12.5 to TrkBCreER;Ai3/Ai9, $n = 4$ animals), Aβ Field-LTMRs (2 mg at E16.5 to $TrkC^{CreER}$;Ai3/Ai9, $n = 3$ animals), Aβ SAI-LTMRs (2 mg at E12.5 to $TrkC^{CreER}$;Ai3/Ai9, $n = 3$ animals), and Aβ RA-LTMRs (2 mg at E11.5 to E12.5 to Ret^{CreER}Ai3/Ai9, $n = 3$ animals). For comparisons between innervation patterns according to body region or hair follicle type, statistical significance is denoted above bars by brackets. For Aβ SAI-LTMRs: Two-way ANOVA: $P < 0.0001$, $F(6, 30) = 18.99$. For Aβ Field-LTMRs: two-way ANOVA: $P < 0.0001$, $F(4, 21) = 72.79$. For Aβ RA-LTMRs: two-way ANOVA: $P < 0.0001$, $F(4, 18) = 38.97$. Post hoc Tukey's test: $*P < 0.05$, $**P < 0.01$, $***P < 0.0005$, $****P < 0.0001$.

tamoxifen dosage achieved sparse labeling of individual neurons for each LTMR subtype (Fig. 4). We used this LTMR sparse labeling strategy to determine the number of axonal branches of the same individual LTMR that innervates a single hair follicle (Fig. 4). This analysis focused on C-LTMRs, Aδ-LTMRs, Aβ RA-LTMRs, and Aβ Field-LTMRs, but not Aβ SA-LTMRs, because these LTMR subtypes exhibit endings that typically associate with many hair follicles, whereas Aβ SA-LTMRs typically innervate only one Merkel cell complex, or touch dome, associated with one guard hair. Interestingly, while individual Aδ-LTMRs, Aβ RA-LTMRs, and Aβ Field-LTMRs have nearly entirely nonoverlapping patterns of hair follicle innervation (Fig. 4 *B–E*), more than 72.4% of the hair follicles innervated by C-LTMRs displayed a multiple-axon branch innervation pattern (Fig. 4 *A* and *E*). Aβ Field-LTMRs exhibit the lowest percentage of multiple-axonal isoneuronal innervation of hair follicles, with only 1.2% of hair follicles innervated by multiple axons from the same Aβ Field-LTMR (Fig. 4 *C* and *E*). Thus, isoneuronal cutaneous processes of three of four LTMRs exhibit minimal overlap, indicative of self-avoidance.

Together, these findings reveal four basic features of LTMR innervation of hairy skin. (*i*) Two LTMRs of the same class rarely innervate the same hair follicle, with the exception of Aβ RA-LTMRs; therefore, most LTMRs are largely tiled with respect to hair follicles. (*ii*) While individual LTMRs within most classes do not overlap with respect to hair follicles, they may innervate hair follicles that are intermingled within a skin region. Aβ Field-LTMRs are the most prominent example of this. (*iii*) The extent of innervation overlap for neurons of the same LTMR class differs, albeit subtly, according to body region and hair follicle type. (*iv*) LTMRs are mostly isoneuronally nonoverlapping with respect to the hair follicles they innervate, probably the result of developmental self-avoidance, with C-LTMRs being the sole exception to this rule.

LTMR Subtypes Exhibit Disproportionate Central Elongation Along the Rostrocaudal Axis of the Spinal Cord. Sparse labeling of LTMR subtypes also afforded a simple method for comparing and contrasting the central projection patterns of individual neurons of each of the five hairy skin LTMR classes, with respect to size and shape of their peripheral projections. We first noticed that none of the five LTMR subtypes exhibit a bias in the rostrocaudal or mediolateral distribution of their endings in the skin (Figs. 4 *A–D* and 5), even though individual neurons of each LTMR subtype innervate a different number of hair follicles and total skin area (6). Second, consistent with prior work (1), sparse labeling also revealed that the central axonal projections of LTMR subtypes exhibit extensive elongation along the rostrocaudal dimension of the spinal cord (Fig. 5). Thus, comparing these peripheral and central axonal projection patterns of C-LTMRs, Aδ-LTMRs, and Aβ RA-LTMRs, we find that the central projections of each LTMR subtype occupied an area in the spinal cord that extends considerably longer along the rostrocaudal axis and much less along the mediolateral axis compared with that of its corresponding cutaneous receptive field (Fig. 5*B*). Indeed, rostrocaudal:mediolateral ratios of the central

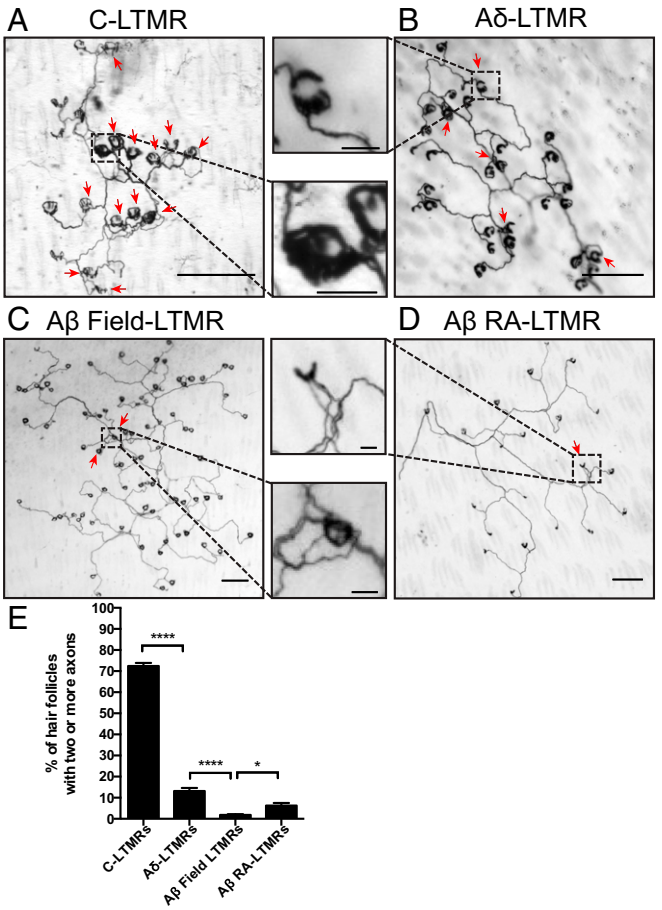

Fig. 4. Individual LTMR peripheral axonal branches innervating hair follicles are largely nonoverlapping, with the exception of C-LTMRs. Representative images from hairy skin whole-mount AP staining of sparsely labeled (*A*) C-LTMRs, (*B*) Aδ-LTMRs, (*C*) Aβ Field-LTMRs, and (*D*) Aβ RA-LTMRs. (Scale bars, 200 μm; *Insets*, 30 μm.) (*E*) Quantifications of isoneuronal axonal overlap within individual LTMR receptive fields. C-LTMRs [1 mg at P12 to $TH^{2A\text{-}CreER}$;$Brn3a^{f(AP)}$; $n = 32$ neurons], Aδ-LTMRs [0.001 mg at P10 to $TrkB^{CreER}$;$Brn3a^{f(AP)}$; $n = 26$ neurons], Aβ Field-LTMRs [0.01 mg at P8 to $TrkC^{CreER}$;$Brn3a^{f(AP)}$; $n = 26$ neurons], Aβ RA-LTMRs [0.03 mg at E11.5 to Ret^{CreER}; $Brn3a^{f(AP)}$; $n = 35$ neurons]. Bars represent the relative fraction of innervated hair follicles that receive innervation by multiple axonal branches of individual neurons for each LTMR subtype. Red arrows indicate hair follicles that are innervated by multiple axons. One-way ANOVA: $*P < 0.05$, $****P < 0.0001$.

projections of individual C-LTMRS are ∼15:1, Aδ-LTMRs are ∼20:1, and Aβ-LTMR subtypes are as much as 40:1 (Fig. 5*B*). This is striking because the rostrocaudal:mediolateral ratio of adult mouse trunk hairy skin, when considered as a 2D sheet, is ∼1:0.75, while that of the spinal cord is ∼10:1. These findings are consistent with the notion that the central circuits engaged by LTMRs are disproportionately oriented along the rostrocaudal axis. Also consistent with this, the dendrites of many, if not most, LTMR-RZ interneuron and projection neuron populations show greater elongation along the rostrocaudal than the mediolateral axis of the spinal cord (27, 35).

LTMR Central Projections Exhibit Body-Region–Specific Central Projection Patterns. We next asked the more challenging question of whether LTMR central projection patterns vary for individual neurons that innervate different body regions. To address this, we needed to develop a method to label the central projections of individual LTMRs in a somatotopically relevant manner. We required an LTMR labeling strategy in which: (*i*) LTMR subtypes are sparsely and specifically labeled; (*ii*) genetic labeling is achieved for neurons innervating a particular body region such that only LTMRs with adjacent or overlapping peripheral receptive fields are labeled; and (*iii*) both peripheral and central projections of LTMRs can be visualized. For this purpose, we combined the use of LTMR-Cre and -CreER lines (Fig. 1 and *SI Appendix*, Table S1) with two dual-recombinase-dependent fluorescent reporters [$R26^{LSL\text{-}FSF\text{-}JAWS\text{-}GFP}$ (Ai57) and $R26^{LSL\text{-}FSF\text{-}TdTom}$ (Ai65)] (36) and skin injections of adeno-associated virus (AAV)-FlpO to sparsely label select subtypes of LTMRs innervating the same small region of hairy skin with distinct reporters.

We first screened a large number of AAV serotypes for one with optimal tropism for LTMRs following skin injection (37–39). While the efficiency of certain AAV serotypes for gene delivery directly to DRG neurons had been previously reported (40, 41), we sought to identify serotypes suitable for labeling DRG neurons via local skin injections. A panel of AAV constructs (*SI Appendix*, Table S2) (University of Pennsylvania Vector Core) (36) were tested for labeling efficiency. This analysis revealed AAV1 as an efficient AAV serotype for labeling DRG neurons via skin injection (*SI Appendix*, Fig. S2).

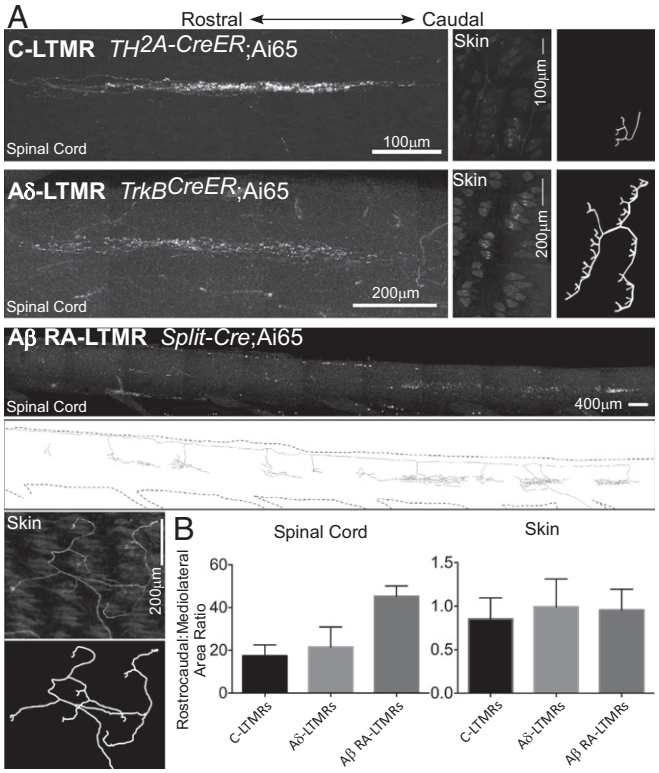

Fig. 5. LTMR central projections show rostrocaudal elongation and mediolateral compression compared with their peripheral projections. (*A*) Representative images of whole-mount stain of spinal cord dorsal horn and back hairy skin to target C-LTMRs, Aδ-LTMRs, and Aβ RA-LTMRs. C-LTMRs are labeled using $TH^{2A\text{-}CreER}$; Ai65 and 500 nL AAV1-Syn-FlpO injection to back hairy skin at P7 and 0.5 mg tamoxifen at P21. Aδ-LTMRs are labeled using $TrkB^{CreER}$; Ai65 with 250 nL AAV-Syn-FlpO injection to back hairy skin at P12 and 2 mg tamoxifen at P21. Aβ RA-LTMRs are labeled using Split-Cre;Ai65 with 250 nL AAV-Syn-FlpO injection to back hairy skin at P11. Images are compressed *z*-projections. Scale, as well as relative rostrocaudal orientation, are indicated. Reconstructions of skin images are displayed for all three subtypes, as well as for the Aβ RA-LTMR spinal cord image. (*B*) Quantification of rostrocaudal:mediolateral ratio of area occupied by individual C-, Aδ-, and Aβ RA-LTMRs in spinal cord (*Left*) versus hairy skin (*Right*) ($n = 21$, 15, and 25 neurons for C-LTMRs, Aδ-LTMRs, and Aβ RA-LTMRs, respectively).

The viral construct used for all subsequent skin injections was AAV2/1-humanSynapsin1-FlpO (AAV1-Syn-FlpO) (*SI Appendix*, Table S2) (36). To visualize LTMR projections within the spinal cord or brainstem, we tested published whole-mount clearing methods, including Scale (42), ClearT and ClearT2 (43), CLARITY (44), and iDISCO (45), as well as modified versions of existing fluorescent staining protocols and BABB (1 part benzyl alcohol: 2 parts benzyl benzoate) clearing (*SI Appendix*, *Experimental Procedures*). We found that a modified whole-mount fluorescent staining protocol employing BABB clearing was optimal for visualizing the central projections of fluorescently labeled LTMRs (*SI Appendix*, *Experimental Procedures* and Fig. S3). We also optimized the timing and volume of viral injections using this AAV construct for each LTMR subtype (*SI Appendix*, Table S3).

We first used AAV1-Syn-FlpO virus injections into different skin regions of LTMR-Cre or -CreER and dual-recombinase reporter mice to assess the central projection patterns of individual neurons for each LTMR class. We observed that there are indeed body-region–specific differences in the central projection patterns of LTMR subtypes. This is best illustrated when comparing LTMRs that innervate thoracic back hairy skin and those that innervate cervical or thoracic abdominal hairy skin. We observed that central projections of C-LTMRs, Aδ-LTMRs, and Aβ RA-LTMRs innervating back hairy skin consistently terminated in a more rostral location relative to the DRG in which their cell body resides (Fig. 6*B*), consistent with previous work (35). This same pattern was observed for lumbar back and thigh hairy skin-innervating neurons. Conversely, the central projections of LTMRs that innervate cervical or thoracic abdominal skin instead exhibited a bias in the caudal direction (Fig. 6). Specifically, the central axons of abdominal C-LTMRs and Aδ-LTMRs project caudally from their dorsal root of entry into the spinal cord. Abdomen-innervating Aβ RA-LTMRs, like all Aβ-LTMRs, were observed to bifurcate and send collaterals in both directions; however, abdominal hairy skin Aβ RA-LTMRs have more collaterals located caudal to the cell body, compared with their back hairy skin counterparts, which display a greater number of collaterals rostral to the cell body (Fig. 6*B*). Curiously, abdominal Aβ RA-LTMRs are distinguished from other Aβ-LTMRs in that they do not have a central projection that ascends via the dorsal column to the dorsal column nuclei (DCN; three of three neurons analyzed). This indicates that signals emanating from abdominal body region LTMRs must be conveyed to the brain via spinal cord projection neurons. Together, these findings reveal fundamental differences in morphological and anatomical properties of LTMR central projections based on body region and location of their cutaneous receptive fields.

LTMR Central Projections Exhibit a Remarkably High Degree of Topographic Adjacency and Subtype-Specific Projection Patterns. A key feature of the mechanosensory system is that the CNS is topographically organized with respect to the periphery. The central projections of LTMRs are somatotopically organized such that body maps exist in the spinal cord and brainstem, tectum, thalamus, and somatosensory cortex (20–22). Genetic labeling of the central axonal projections of two or more LTMRs

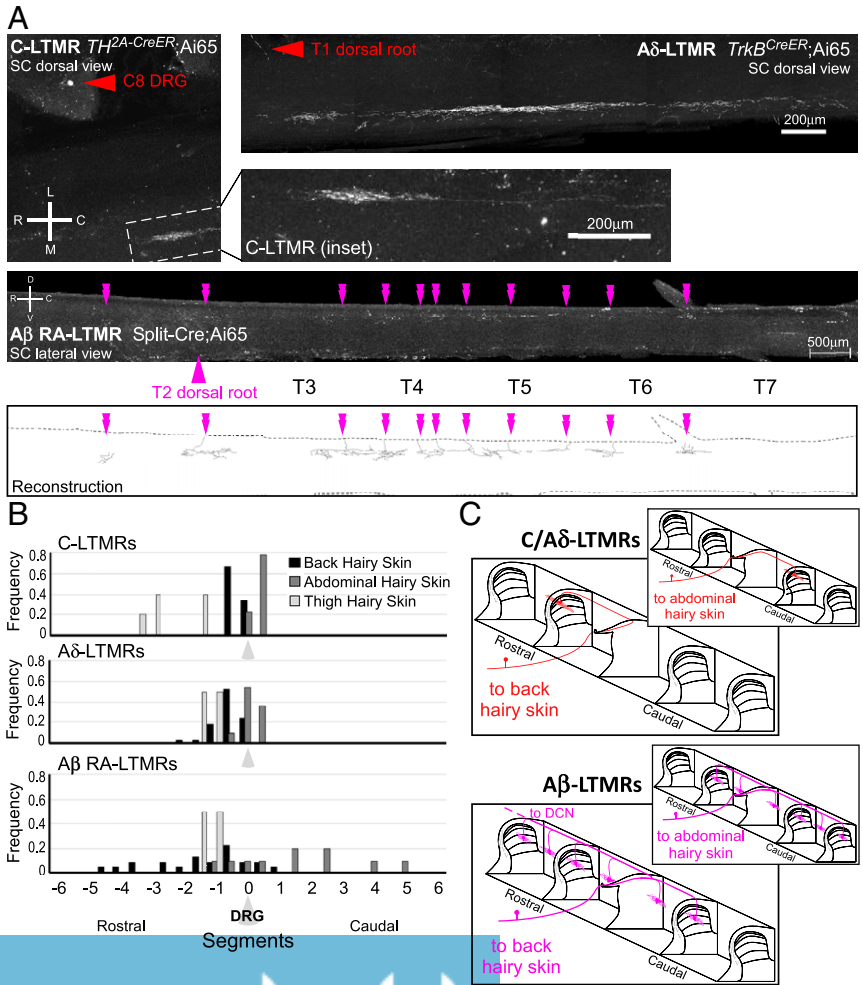

Fig. 6. LTMR central projection display morphological differences according to body region innervated. (*A*) Representative images of whole-mount immunostained spinal cords showing LTMRs that innervate abdominal hairy skin. C-LTMRs were labeled using $TH^{2A\text{-}CreER}$; Ai65 with 500 nL AAV1-Syn-FlpO injection into abdominal hairy skin at P7 and 0.5 mg tamoxifen at P21. *Inset* shows full central projection; red arrowhead labels corresponding soma in C8 DRG. Aδ-LTMRs were labeled using $TrkB^{CreER}$; Ai65 with 250 nL AAV1-Syn-FlpO injection into abdominal hairy skin at P10 and 2 mg tamoxifen at P21. Red arrowhead labels corresponding axon entry (soma in T1 DRG). Aβ RA-LTMRs are labeled using Split-Cre; Ai65 with 200 nL AAV-Syn-FlpO injection into abdominal hairy skin at P10. Purple arrowhead indicates dorsal root of entry (soma in T2 DRG); double arrowheads denote collaterals in the spinal cord. Images are compressed *z*-projections. Scale, rostrocaudal (R, C), mediolateral (M, L), and dorsoventral (D, V) axes are indicated. Reconstruction for the Aβ RA-LTMR image is displayed. (*B*) Quantification of collateral location relative to soma-containing DRG, according to body region innervated (back hairy skin, black; abdomen hairy skin, dark gray; thigh hairy skin, light gray). C-LTMRs $n = 17$; Aδ-LTMRs $n = 49$; Aβ RA-LTMRs $n = 5$. (*C*) Schematic depicting unique central projection organization for LTMRs innervating back vs. abdominal hairy skin (not to scale).

within the same LTMR class afforded an opportunity to define the precise spatial relationships of the central axonal projections of two or more individual LTMRs whose terminations within the skin are adjacent or overlapping, as described above. Therefore, we developed a strategy using AAV1-Syn-FlpO skin injections into small regions of the skin of mice harboring one LTMR-CreER allele and two dual recombinase-dependent fluorescent reporter alleles (Ai65 and Ai57) (36) to achieve stochastic labeling via one or both fluorescent reporters of a few neurons of the same class. This strategy allowed us to visualize the relative locations of the spinal cord projections of two or more LTMRs of the same class that have adjacent or overlapping cutaneous receptive fields. For this analysis, we focused on the C-LTMRs, Aδ-LTMRs, and one Aβ-LTMR subtype, Aβ RA-LTMRs. We observed that, for neurons innervating the same small region of skin, labeled cell bodies were widely and seemingly randomly distributed throughout individual ganglia, and occasionally in adjacent ganglia, and yet the spinal cord projections were either immediately adjacent or overlapping with each other (Fig. 7). Two C-LTMRs, whose cutaneous receptive fields are predominantly nonoverlapping (i.e., tiled), exhibited central projections within the spinal cord that are immediately adjacent to one another, with remarkably little or no overlap (Fig. 7*A*). The central projections of Aδ-LTMRs, which also tile the skin, also showed remarkable topographic adjacency, but with a slightly higher degree of overlap in both the rostrocaudal and mediolateral axes (Fig. 7*B*). Similarly, the central projections of Aβ RA-LTMRs, whose peripheral projections often overlap with respect to both hair follicles innervated and, to a lesser extent, skin region (i.e., not strictly tiled) and whose central projections exhibit expansive collaterals rostrocaudally within the spinal cord, also showed topographic overlap or adjacency (Fig. 7*C*).

Two general principles emerge from these findings. First, the cell bodies of LTMR subtypes that innervate overlapping or adjacent skin regions are distributed in a seemingly random manner within the DRG, and in some cases in different DRGs, yet their central terminals in the spinal cord exhibit a striking degree of topographic overlap or adjacency. Second, the central axonal projections of different LTMR subtypes exhibit varying degrees of spatial overlap or adjacency. C-LTMRs are most impressive in that they display immediately adjacent dorsal horn termination patterns, with virtually no overlap, while the two other hairy skin lanceolate-ending LTMR subtypes, Aδ-LTMRs and Aβ RA-LTMRs, have varying degrees of overlap. Thus, hairy skin LTMR subtypes differ not only in their physiological properties, peripheral and central axonal morphologies, and the numbers and types of hair follicles they innervate, they are also distinguished by their tiling patterns in the skin and the organization and extent of topographic alignment or adjacency of their central axonal projections.

Discussion

The tactile sensory system allows us to localize, perceive, and react to different types of complex mechanical stimuli acting on the body, and it is therefore essential that impulses carried by LTMRs that convey distinct modalities of touch are integrated within the CNS in a somatotopically relevant manner. The functional organization of tactile sensory circuits for murine hairy skin begins with a precise, invariant pattern of five or more LTMR subtype endings associated with three main hair follicle types and an iterative spatial distribution of these hair follicles across the body. Findings presented here reveal the tiling patterns and isoneuronal morphological properties of hairy skin LTMR subtypes, including variations across the body surface, and a sharp precision with which LTMR subtype central terminations are somatotopically aligned within the spinal cord. These findings extend our appreciation of the functional organization of the hairy skin tactile sensory system and the dorsal horn as a locus of LTMR subtype integration for tactile information processing.

Implications of LTMR Peripheral Innervation Patterns and Organization. Each hairy skin LTMR subtype exhibits a unique combination of features that govern its responses to mechanical stimuli to ultimately influence behavioral reactions to, and perception of, the physical world. Features that distinguish the five hairy skin LTMR subtypes include: patterns of association with peripheral end organs, such as hair follicle types or Merkel cells; the number and distribution of axonal endings in the skin; action potential conduction velocities, sensitivities, and rates of adaptation to sustained skin indentation; central projection patterns and postsynaptic partners; and the modulation of CNS terminals by inhibitory axo-axonic synapses (1, 2, 27, 46). Knowing the organizational properties, including the spacing and degree of overlap of individual LTMR cutaneous endings in the skin, is informative for understanding how mechanical forces acting on the skin are represented and integrated within the CNS.

We found that the majority of LTMRs within a particular class terminate within trunk hairy skin in a manner that is largely nonoverlapping or tiled, and therefore, an individual LTMR within most classes occupies its own unique territory. In this sense, the mammalian tactile sensory system exhibits organizational features common to at least some other sensory systems, where neurons avoid innervating territories occupied by other neurons of the same functional class. Indeed, tiling has been observed in many types of neurons, including leech and *Drosophila* mechanosensory neurons (14, 47), and mammalian retinal ganglion cells (48–50). This organizational feature enables maximal coverage of sensory space with minimal redundancy (11), which would be metabolically costly (51, 52). Tiling of LTMRs within a class may also enable definition of central somatotopic maps and is perhaps an essential anatomical substrate of spatial acuity. A further implication of LTMR tiling observed here is that individual neurons of a tiled LTMR population perform the same function, as has been shown in other systems and organisms. This is an important notion because the high degree of tiling observed for four of the five hairy skin LTMR populations makes a compelling case that the genetic tools used for these LTMR populations indeed label functionally irreducible neuronal populations.

One notable observation from our population morphological receptive field analyses is that Aβ RA-LTMRs are distinguished from the other four hairy skin LTMR subtypes in that they are not tiled. That is, hair follicles are frequently innervated by two, and in the case of guard hairs up to three Aβ RA-LTMRs, which were genetically labeled using Ret^{CreER} mice. At least two possibilities may explain this observation. First is that all of the Aβ RA-LTMRs labeled using Ret^{CreER} are functionally similar or identical and this seemingly redundant or overlapping innervation pattern reflects unique properties of the large hair follicles types and the functions they subserve. The guard hairs have large diameter follicles and the longest hair shafts, which may allow them to detect the slightest deflections during animal movement or in response to stimuli acting on their hair shaft tips, far away from the body surface. Thus, guard hairs may be viewed as unique in somatosensation because they enable the sense of touch to extend far away from the surface of the skin. As such, our observation that two or three Aβ RA-LTMRs innervate each guard hair may suggest a greater need for at least one of them being active at submaximal stimulation thresholds. A second possibility is that our genetic labeling strategy using Ret^{CreER} mice (28) may label two functionally distinct Aβ RA-LTMR populations that are themselves homotypically tiled. In this scenario, there would exist two distinct Aβ RA-LTMR populations with distinguishing features not apparent in physiological and anatomical analyses done to date. We find this idea to be

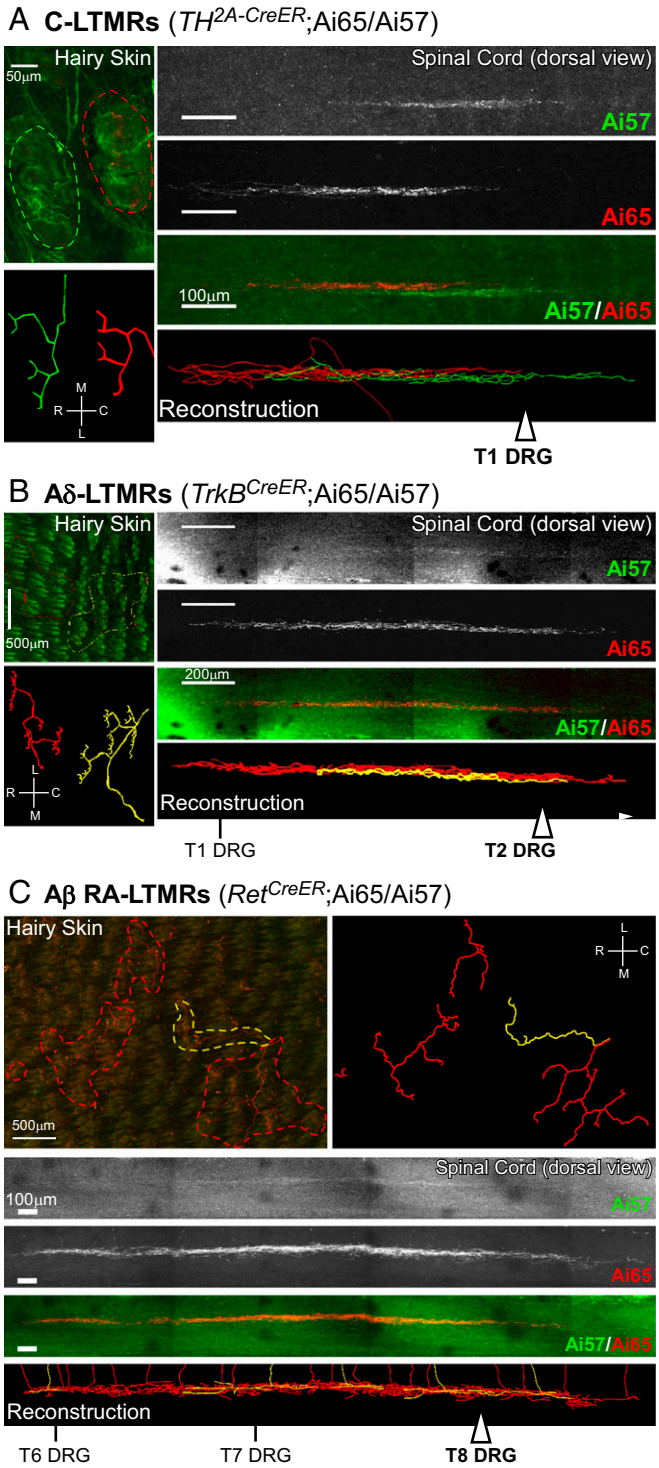

Fig. 7. Central projection alignment and overlap patterns of homotypic LTMR subtypes. Representative images from back hairy skin and spinal cord whole-mount fluorescence staining. (*A*) C-LTMRs ($n = 3$ animals), for which a green neuron and a red neuron are labeled; (*B*) Aδ-LTMRs ($n = 4$ animals), for which a red neuron and a yellow neuron are labeled; and (*C*) Aβ RA-LTMRs ($n = 3$ animals), for which four red neurons and a yellow neuron are labeled. Injections of AAV1-Syn-FlpO virus into the skin of LTMR-CreER; Ai65/57 animals labeled a small number of LTMRs; individual LTMRs were labeled with tdTomato (Ai65), GFP (Ai57), or both reporters. See *SI Appendix*, Table S2 for AAV1-Syn-FlpO and tamoxifen dosages for targeting of each LTMR subtype. Outline of skin innervation patterns are depicted, in addition to reconstructions (*SI Appendix*, *Experimental Procedures*) to showcase innervation pattern. Reconstructions are also displayed for the spinal cord projections. White arrowheads mark dorsal root entry sites to the spinal cord for DRGs where corresponding cell bodies were located. Scale, as well as relative rostrocaudal (R, C) and mediolateral (M, L) axes, are indicated.

appealing because in the original physiological characterization of hairy skin Aβ RA-LTMRs, made in the cat (5), two distinguishable fast-conducting LTMR subtypes responding to hair deflection and exhibiting rapid adaptation to sustained skin indentation were observed; distinguishing features of the two feline Aβ RA-LTMRs are their receptive field sizes and conduction velocities (5). Therefore, it is tempting to speculate the existence of functionally distinct murine hairy skin Aβ RA-LTMR subtypes, each exhibiting homotypic tiling as we observed for all other LTMR subtypes. Future transcriptome profiling of single Aβ RA-LTMR neurons may address the question of whether there are two distinct subtypes and provide genetic labeling tools to examine whether neurons in each subtype exhibit tiling.

The arrangements of LTMR axonal branches in the skin may shape their responses to mechanical stimuli (for example, ref. 6). One mechanism underlying interaxonal spacing arrangement is self-avoidance, a phenomenon in which axonal branches of the same neuron repel each other to avoid growing into the same territory (12). Self-avoidance has been studied extensively in systems where neuronal arbors innervate a 2D plane, such as the mammalian retina or *Drosophila* larval body wall (11, 12). However, whether mammalian LTMRs exhibit features reflecting developmental self-avoidance had been unknown. Through sparse genetic labeling of single LTMR peripheral projections, we found that isoneuronal branches of most LTMRs in the skin exhibit little overlap with respect to the hair follicles they innervate. While the tendency of minimal overlap between isoneuronal branches is indeed a feature of neurons that exhibit developmental self-avoidance, we refrain from concluding that LTMR axonal branches self-avoid because it is not yet known whether these branches recognize and repel each other during development or whether other, noncell-autonomous mechanisms contribute to the lack of isoneuronal branch overlap. Indeed, it is possible that end organs, such as hair follicles, terminal Schwann cells, or Merkel cells instruct or contribute to the precise spatial arrangements of LTMR axons as they acquire their mature morphologies. Future studies using live imaging of LTMR axonal dynamics during development to assess the behavior of LTMR isoneuronal branches will be needed to determine whether LTMR axons employ self-recognition and self-avoidance mechanisms to achieve isoneuronal spacing patterns described here. Furthermore, we speculate that the isoneuronal arrangements of axonal branches may influence LTMR subtype responses to mechanical stimuli. In the case of C-LTMRs, for example, we speculate that their highly redundant isoneuronal branch hair follicle innervation pattern allows for more sensitive detection of mechanical stimuli acting on awl/auchene and zigzag hairs than would a single branch innervation pattern.

Somatotopic Properties of LTMR Central Projections. Organizational properties of LTMR central projections, revealed in this study, provide clues for how the tactile stimuli acting on a particular region of skin form 3D neural representations in the spinal cord, in a somatotopically relevant manner. The observation that all LTMR classes exhibit dramatically more volumetric expansion along the rostrocaudal axis of the spinal cord, relative to their 2D arrangements in the skin, may reflect anatomical spatial constraints and perhaps a unique computational feature of this system. Consistent with this, dendrites of interneurons of the deep dorsal horn, the majority of which receive input from three or more LTMR subtypes, are more elaborate along the rostrocaudal axis of the spinal cord, compared with their interneuron counterparts in lamina I/II (27, 53). These distinguishing organizational features of the LTMR-recipient zone support a model of

dorsal horn tactile information processing in which postsynaptic partners of LTMRs integrate across multiple LTMR subtypes, which innervate a common area of skin, as opposed to integrating across one LTMR subtype and a large skin area; the latter may be inferred if postsynaptic partners of LTMRs showed more expansive mediolateral dendrites. We propose that expansive coalignment along the spinal cord rostrocaudal axis of the five LTMR subtype terminals and postsynaptic partner neurons reflects a dorsal horn circuit that enables somatotopically precise modality integration. It is noteworthy that the central projections of LTMRs innervating abdominal hairy skin project more caudally than rostrally, again possibly reflecting anatomical space constraints; however, the absence of abdomen-innervating Aβ RA-LTMR projections to the DCN indicates that these LTMRs may engage different circuits than LTMRs innervating other body regions. Indeed, different body regions may be exposed to different tactile cues, and these may engage and possibly require different central circuits.

We found that for C-LTMRs, Aδ-LTMRs, and at least one Aβ-LTMR subtype that innervate the same small region of skin, their central terminals exhibit striking adjacency in the dorsal horn. This is even more remarkable when considering that the cell bodies of somatotopically aligned neurons exhibit no obvious pattern of organization within individual DRGs. Moreover, the central projections of these three classes of LTMRs are distinguished by their "nearest-neighbor" relationships. It is curious, for example, that Aδ-LTMRs and C-LTMRs exhibit different degrees of overlap of their central projections even though the peripheral projection patterns of these two LTMR subtypes are comparable. Both of these LTMR subtypes innervate only zigzag and awl/auchene hairs, display largely nonoverlapping (tiled) peripheral anatomical receptive fields, and are optimally tuned to hair deflection and gentle skin indentation (1, 7). One notable difference, however, is that Aδ-LTMRs have lanceolate endings that are strongly biased to the caudal regions of hair follicles, while C-LTMRs as a population distribute their lanceolate endings more evenly around hair follicles (8), a feature that may be enabled by their high degree of isoneuronal overlap reported here. Because of this, Aδ-LTMRs, but not C-LTMRs, are preferentially sensitive to deflection of body hairs in the caudal-to-rostral direction (8). Thus, we speculate that differences between the central alignment patterns of Aδ-LTMRs and C-LTMRs may reflect functional differences in central processing, perhaps related to directional responses to hair deflection. Regardless, most striking is the extent of somatotopic adjacency of LTMR central projections, which is most easily observed for the Aδ-LTMRs and C-LTMRs because of their relatively compact central termination patterns. This is particularly intriguing for C-LTMRs because these neurons are implicated in affective rather than discriminative touch (54). Why would the central projections of a neuron that does not contribute to spatial acuity be so precisely somatotopically arranged? These considerations make us favor the idea that the remarkably high degree of central projection alignment of the axonal terminations of at least some LTMR subtypes is more a reflection of somatotopically relevant LTMR subtype central integration and processing, perhaps even the extraction of features including direction and speed of movement, and orientation of objects, than with acuity per se, or perceptually relevant spatial discrimination. Perhaps C-LTMRs and Aδ-LTMRs modulate or shape the central processing of inputs from Aβ-LTMR subtypes that do govern acuity (for example, see ref. 27). These and related ideas stemming from the anatomical and morphological analysis of LTMR subtype organization presented here will help to guide future physiological analyses of spinal cord tactile circuits and their mechanisms and functions in touch perception and behavior.

An Emerging View of the Central Representation of Touch. How and where in the CNS are LTMR activity ensembles processed into perceptually relevant codes of neural impulses? Historically, most emphasis has been placed on a "direct DC pathway" model of somatosensation (20, 55–57). In this view, individual LTMR subtypes convey particular modalities of tactile stimuli, including skin indentation, vibration, and stretch, directly to the brainstem DCN of the brainstem, where their signals are then faithfully relayed via the thalamus to the somatosensory cortex. This "labeled line" direct DC pathway model posits that modality integration begins in somatosensory cortex, giving rise to cortical neurons tuned to higher-order features, such as object orientation, direction, and speed of motion, texture, compliance, and shape. Contrary to this prevailing view, however, we previously found that the vast majority of hairy skin LTMR synapses reside within a discrete region of the spinal cord dorsal horn, which we call the LTMR-RZ, with relatively few synapses in the DCN (6–8, 27). In fact, C-LTMRs, Aδ-LTMRs, most caudal-level Aβ SA1-LTMRs, and abdominal Aβ RA-LTMRs, which together account for more than half of all LTMRs, terminate exclusively in the spinal cord LTMR-RZ without an axonal projection to the DCN (6–8, 27). Therefore, any contributions of these LTMR subtypes to the cortical representation of touch, and thus touch perception, must be mediated by spinal neurons situated in the LTMR-RZ. We also found that C-LTMRs, Aδ-LTMRs and Aβ LTMR receptive fields are largely tiled (present study), yet overlap with respect to each other within the same small region of skin (7, 9). Similarly, while the central projections of LTMRs of the same class are highly somatotopically aligned (present study), heterotypically they overlap (7). As such, we propose that somatotopically aligned dorsal horn columns of the LTMR-RZ represent fundamental units of functional organization that process LTMR subtype activity ensembles emanating from the skin (1, 7, 27). LTMR-RZ output pathways that might convey integrated and transformed LTMR activity ensembles include the "indirect DC pathway," which is poorly understood, and the anterolateral tract, which is classically associated with conveying pain and temperature information to the brain (1, 58).

We recently generated a large array of spinal cord dorsal horn genetic tools to interrogate the cellular substrates of LTMR-RZ information processing (27). Our analysis revealed that: (*i*) the LTMR-RZ is highly complex and contains at least 11 morphologically and physiologically distinct interneuron classes; (*ii*) each LTMR subtype forms synapses broadly onto four or more LTMR-RZ interneuron classes; (*iii*) each LTMR-RZ interneuron class receives convergent inputs from two or more LTMR subtypes, cortex, and other LTMR-RZ interneurons; and (*iv*) LTMR-RZ interneurons are essential for both tactile sensitivity and texture discrimination (27). Importantly, the predominance of LTMR synapses localized to the dorsal horn instead of the DCN, the somatotopically arranged convergence of LTMR subtype inputs within the LTMR-RZ, and the remarkably rich cellular and synaptic architecture of this spinal cord region suggest a role as a major sensory processing center, akin to the retina. Our findings in this and previous reports support a view of somatosensation in which modality integration and processing begins in the LTMR-RZ, and we suggest there is much to be learned about the nature of tactile feature representation in both the LTMR-RZ and DCN.

There is a remarkable diversity of touch-sensitive LTMRs, as well as a remarkable diversity of ascending projection systems. Our findings suggest principles of organization within the LTMR-RZ that will constrain and inform efforts to define the functional organization underlying this diversity of inputs and outputs. What is the logic of synaptic organization within the LTMR-RZ, and how are LTMR inputs integrated and propagated via the ascending pathways to the brain? Which stimulus features are represented in spinal and DCN output pathways?

How do direct DC pathway signals integrate with indirect DC pathway signals within the DCN? We propose that these are among the most compelling questions in modern somatosensory research.

Materials and Methods

For a complete description of materials and methods, please refer to *SI Appendix*.

Published reporter mouse lines used for this study included *R26*$^{LSL\text{-}YFP}$ (Ai3) (Jax#007903); *R26*$^{LSL\text{-}tdTomato}$ (Ai9) (Jax#007909); *R26*$^{LSL\text{-}FSF\text{-}TdTom}$ (Ai65) (Jax#021875); *R26*$^{LSL\text{-}FSF\text{-}JAWS\text{-}GFP}$ (Ai57) (36); and *Brn3a*$^{f(AP)}$ (34). LTMR-CreER lines include *TH*$^{2A\text{-}CreER}$ (27), *TrkB*^{CreER} (8), *TrkB*$^{Tau\text{-}GFP}$ (7), *Ret*^{CreER} (28), *TrkC*^{CreER} (6), *Ret*^{fCFP} (59), and Split-Cre (8, 60). Mice were handled and housed in accordance with the Harvard Medical School and Johns Hopkins University Institutional Animal Care and Use Committee guidelines.

ACKNOWLEDGMENTS. We thank Katherine West, Connie Tsan, Katelyn Comeau, and Annie Chen for expert technical support; and D.D.G. laboratory members for discussions and comments on the manuscript. This work was supported by NIH Grants 5R35NS097344-02 (to D.D.G.) and 1F32NS108507-01 (to S.M.); a Hanna Gray fellowship (to S.M.); and the Edward R. and Anne G. Lefler Center for the Study of Neurodegenerative Disorders (D.D.G.). D.D.G. is an investigator of the Howard Hughes Medical Institute.

1. Abraira VE, Ginty DD (2013) The sensory neurons of touch. *Neuron* 79:618–639.
2. Zimmerman A, Bai L, Ginty DD (2014) The gentle touch receptors of mammalian skin. *Science* 346:950–954.
3. Owens DM, Lumpkin EA (2014) Diversification and specialization of touch receptors in skin. *Cold Spring Harb Perspect Med* 4:a013656.
4. Horch KW, Tuckett RP, Burgess PR (1977) A key to the classification of cutaneous mechanoreceptors. *J Invest Dermatol* 69:75–82.
5. Burgess PR, Petit D, Warren RM (1968) Receptor types in cat hairy skin supplied by myelinated fibers. *J Neurophysiol* 31:833–848.
6. Bai L, et al. (2015) Genetic identification of an expansive mechanoreceptor sensitive to skin stroking. *Cell* 163:1783–1795.
7. Li L, et al. (2011) The functional organization of cutaneous low-threshold mechanosensory neurons. *Cell* 147:1615–1627.
8. Rutlin M, et al. (2014) The cellular and molecular basis of direction selectivity of Aδ-LTMRs. *Cell* 159:1640–1651, and erratum (2015) 160:1027.
9. Li L, Ginty DD (2014) The structure and organization of lanceolate mechanosensory complexes at mouse hair follicles. *eLife* 3:e01901.
10. Ghitani N, et al. (2017) Specialized mechanosensory nociceptors mediating rapid responses to hair pull. *Neuron* 95:944–954.e4.
11. Grueber WB, Sagasti A (2010) Self-avoidance and tiling: Mechanisms of dendrite and axon spacing. *Cold Spring Harb Perspect Biol* 2:a001750.
12. Zipursky SL, Grueber WB (2013) The molecular basis of self-avoidance. *Annu Rev Neurosci* 36:547–568.
13. Shrestha BR, Grueber WB (2010) Neuronal morphogenesis: Worms get an EFF in dendritic arborization. *Curr Biol* 20:R673–R675.
14. Grueber WB, Jan LY, Jan YN (2002) Tiling of the Drosophila epidermis by multidendritic sensory neurons. *Development* 129:2867–2878.
15. Gallegos ME, Bargmann CI (2004) Mechanosensory neurite termination and tiling depend on SAX-2 and the SAX-1 kinase. *Neuron* 44:239–249.
16. Millard SS, Flanagan JJ, Pappu KS, Wu W, Zipursky SL (2007) Dscam2 mediates axonal tiling in the Drosophila visual system. *Nature* 447:720–724.
17. Lefebvre JL, Kostadinov D, Chen WV, Maniatis T, Sanes JR (2012) Protocadherins mediate dendritic self-avoidance in the mammalian nervous system. *Nature* 488:517–521.
18. Sdrulla AD, Linden DJ (2006) Dynamic imaging of cerebellar Purkinje cells reveals a population of filopodia which cross-link dendrites during early postnatal development. *Cerebellum* 5:105–115.
19. Singhania A, Grueber WB (2014) Development of the embryonic and larval peripheral nervous system of Drosophila. *Wiley Interdiscip Rev Dev Biol* 3:193–210.
20. Mountcastle VB (1957) Modality and topographic properties of single neurons of cat's somatic sensory cortex. *J Neurophysiol* 20:408–434.
21. Kaas JH, Nelson RJ, Sur M, Lin CS, Merzenich MM (1979) Multiple representations of the body within the primary somatosensory cortex of primates. *Science* 204:521–523.
22. Kaas JH (1997) Topographic maps are fundamental to sensory processing. *Brain Res Bull* 44:107–112.
23. Penfield W, Boldrey E (1937) Somatic motor and sensory representation in the cerebral cortex of man as studied by electrical stimulation. *Brain* 60:389–443.
24. Harding-Forrester S, Feldman DE (2018) Somatosensory maps. *Handb Clin Neurol* 151:73–102.
25. Woolf CJ, Fitzgerald M (1986) Somatotopic organization of cutaneous afferent terminals and dorsal horn neuronal receptive fields in the superficial and deep laminae of the rat lumbar spinal cord. *J Comp Neurol* 251:517–531.
26. Brown AG (1982) The dorsal horn of the spinal cord. *Q J Exp Physiol* 67:193–212.
27. Abraira VE, et al. (2017) The cellular and synaptic architecture of the mechanosensory dorsal horn. *Cell* 168:295–310.e19.
28. Luo W, Enomoto H, Rice FL, Milbrandt J, Ginty DD (2009) Molecular identification of rapidly adapting mechanoreceptors and their developmental dependence on ret signaling. *Neuron* 64:841–856.
29. Liu Y, et al. (2012) Sexually dimorphic BDNF signaling directs sensory innervation of the mammary gland. *Science* 338:1357–1360.
30. Madisen L, et al. (2010) A robust and high-throughput Cre reporting and characterization system for the whole mouse brain. *Nat Neurosci* 13:133–140.
31. Cua AB, Wilhelm KP, Maibach HI (1990) Elastic properties of human skin: Relation to age, sex, and anatomical region. *Arch Dermatol Res* 282:283–288.
32. Yosipovitch G, Maayan-Metzger A, Merlob P, Sirota L (2000) Skin barrier properties in different body areas in neonates. *Pediatrics* 106:105–108.
33. Choudhry R, Hodgins MB, Van der Kwast TH, Brinkmann AO, Boersma WJA (1992) Localization of androgen receptors in human skin by immunohistochemistry: Implications for the hormonal regulation of hair growth, sebaceous glands and sweat glands. *J Endocrinol* 133:467–475.
34. Badea TC, et al. (2009) New mouse lines for the analysis of neuronal morphology using CreER(T)/loxP-directed sparse labeling. *PLoS One* 4:e7859.
35. Brown AG (2012) *Organization in the Spinal Cord: The Anatomy and Physiology of Identified Neurones* (Springer Science & Business Media, New York).
36. Madisen L, et al. (2015) Transgenic mice for intersectional targeting of neural sensors and effectors with high specificity and performance. *Neuron* 85:942–958.
37. Zincarelli C, Soltys S, Rengo G, Rabinowitz JE (2008) Analysis of AAV serotypes 1-9 mediated gene expression and tropism in mice after systemic injection. *Mol Ther* 16:1073–1080.
38. Burger C, et al. (2004) Recombinant AAV viral vectors pseudotyped with viral capsids from serotypes 1, 2, and 5 display differential efficiency and cell tropism after delivery to different regions of the central nervous system. *Mol Ther* 10:302–317.
39. Aschauer DF, Kreuz S, Rumpel S (2013) Analysis of transduction efficiency, tropism and axonal transport of AAV serotypes 1, 2, 5, 6, 8 and 9 in the mouse brain. *PLoS One* 8:e76310.
40. Mason MRJ, et al. (2010) Comparison of AAV serotypes for gene delivery to dorsal root ganglion neurons. *Mol Ther* 18:715–724.
41. Vrontou S, Wong AM, Rau KK, Koerber HR, Anderson DJ (2013) Genetic identification of C fibres that detect massage-like stroking of hairy skin in vivo. *Nature* 493:669–673.
42. Hama H, et al. (2011) Scale: A chemical approach for fluorescence imaging and reconstruction of transparent mouse brain. *Nat Neurosci* 14:1481–1488.
43. Kuwajima T, et al. (2013) ClearT: A detergent- and solvent-free clearing method for neuronal and non-neuronal tissue. *Development* 140:1364–1368.
44. Chung K, Deisseroth K (2013) CLARITY for mapping the nervous system. *Nat Methods* 10:508–513.
45. Renier N, et al. (2014) iDISCO: A simple, rapid method to immunolabel large tissue samples for volume imaging. *Cell* 159:896–910.
46. Lumpkin EA, Marshall KL, Nelson AM (2010) The cell biology of touch. *J Cell Biol* 191:237–248.
47. Kramer AP, Kuwada JY (1983) Formation of the receptive fields of leech mechanosensory neurons during embryonic development. *J Neurosci* 3:2474–2486.
48. Dacey DM (1993) The mosaic of midget ganglion cells in the human retina. *J Neurosci* 13:5334–5355.
49. Wässle H, Peichl L, Boycott BB (1981) Dendritic territories of cat retinal ganglion cells. *Nature* 292:344–345.
50. Wässle H, Riemann HJ (1978) The mosaic of nerve cells in the mammalian retina. *Proc R Soc Lond B Biol Sci* 200:441–461.
51. Barlow HB (2012) Possible principles underlying the transformations of sensory messages. *Sensory Communication*, ed Rosenblith WA (MIT Press, Cambridge, MA), pp 216–234.
52. Barlow H (2001) Redundancy reduction revisited. *Network* 12:241–253.
53. Yasaka T, Tiong SYX, Hughes DI, Riddell JS, Todd AJ (2010) Populations of inhibitory and excitatory interneurons in lamina II of the adult rat spinal dorsal horn revealed by a combined electrophysiological and anatomical approach. *Pain* 151:475–488.
54. McGlone F, Wessberg J, Olausson H (2014) Discriminative and affective touch: Sensing and feeling. *Neuron* 82:737–755.
55. Johnson KO, Hsiao SS (1992) Neural mechanisms of tactual form and texture perception. *Annu Rev Neurosci* 15:227–250.
56. Johnson KO, Yoshioka T, Vega-Bermudez F (2000) Tactile functions of mechanoreceptive afferents innervating the hand. *J Clin Neurophysiol* 17:539–558.
57. Johnson KO (2001) The roles and functions of cutaneous mechanoreceptors. *Curr Opin Neurobiol* 11:455–461.
58. Todd AJ (2010) Neuronal circuitry for pain processing in the dorsal horn. *Nat Rev Neurosci* 11:823–836.
59. Uesaka T, Nagashimada M, Yonemura S, Enomoto H (2008) Diminished Ret expression compromises neuronal survival in the colon and causes intestinal aganglionosis in mice. *J Clin Invest* 118:1890–1898.
60. Fleming MS, et al. (2016) A RET-ER81-NRG1 signaling pathway drives the development of pacinian corpuscles. *J Neurosci* 36:10337–10355.